Atmospheric Environment 176 (2018) 91–102

Contents lists available at ScienceDirect

Atmospheric Environment

journal homepage: www.elsevier.com/locate/atmosenv

# Atmospheric depositions of natural and anthropogenic trace elements on the Guliya ice cap (northwestern Tibetan Plateau) during the last 340 years

M. Roxana Sierra-Hernández[a,*], Paolo Gabrielli[a,b], Emilie Beaudon[a], Anna Wegner[a], Lonnie G. Thompson[a,b]

[a] Byrd Polar and Climate Research Center, The Ohio State University, Columbus, OH 43210, United States
[b] School of Earth Sciences, The Ohio State University, Columbus, OH 43210, United States

## GRAPHICAL ABSTRACT

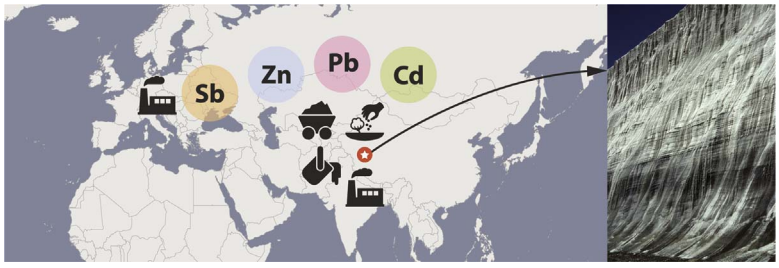


## ARTICLE INFO

*Keywords:*
Atmospheric pollution
Coal combustion
Heavy metals
Fossil fuel
Tibet
Ice core

## ABSTRACT

A continuous record of 29 trace elements (TEs) has been constructed between 1650 and 1991 CE (Common Era) from an ice core retrieved in 1992 from the Guliya ice cap, on the northwestern Tibetan Plateau. Enrichments of Pb, Cd, Zn and Sb were detected during the second half of the 19th century and the first half of the 20th century (~1850–1950) while enrichments of Sn (1965–1991), Cd and Pb (1975–1991) were detected during the second half of the 20th century. The EFs increased significantly by 20% for Cd and Sb, and by 10% for Pb and Zn during 1850–1950 relative to the pre-1850s. Comparisons of the Guliya TEs data with other ice core-derived and production/consumption data suggest that Northern Hemisphere coal combustion (primarily in Western Europe) is the likely source of Pb, Cd, Zn, and Sb during the 1850–1950 period. Coal combustion in Europe declined as oil replaced coal as the primary energy source. The European shift from coal to oil may have contributed to the observed Sn enrichment in ~1965 (60% EF increase in 1975–1991), although regional fossil fuel combustion (coal and leaded gasoline) from western China, Central Asia, and South Asia (India, Nepal), as well as Sn mining/smelting in Central Asia, may also be possible sources. The post-1975 Cd and Pb enrichments (40% and 20% EF increase respectively in 1975–1991) may reflect emissions from phosphate fertilizers, fossil fuel combustion, and/or non-ferrous metal production, from western China, Central Asia, and/or South Asia. Leaded gasoline is likely to have also contributed to the post-1975 Pb enrichment observed in this record. The results strongly suggest that the Guliya ice cap has recorded long-distance emissions from coal combustion since the 1850s with more recent contributions from regional agriculture, mining, and/or fossil fuel combustion. This new Guliya ice core record of TEs fills a geographical gap in the reconstruction of the pollution history of this region that extends well beyond modern instrumental records.

* Corresponding author.
*E-mail address:* sierra-hernandez.1@osu.edu (M.R. Sierra-Hernández).

https://doi.org/10.1016/j.atmosenv.2017.11.040
Received 5 August 2017; Received in revised form 20 November 2017; Accepted 23 November 2017
Available online 08 December 2017

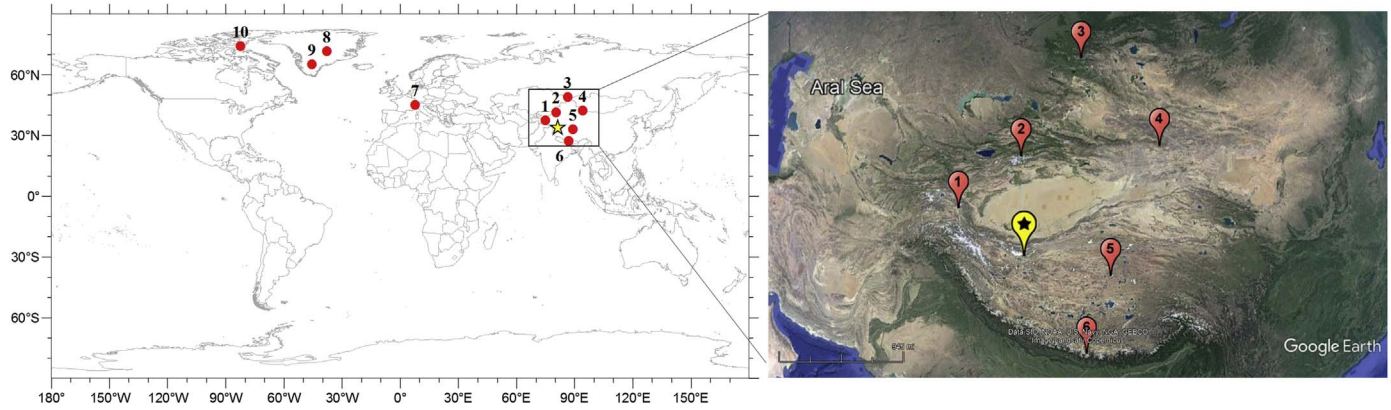


**Fig. 1.** Left: Map showing the locations of the Guliya Ice Cap (star) and other ice cores discussed in the text: 1. Muztagh Ata (East Pamirs); 2. Inilchek (Tien Shan); 3. Belukha (Siberian Altai); 4. Miaoergou (Eastern Tien Shan); 5. Puruogangri (Central Tibet); 6. Everest (Himalayas); 7. Colle Gnifetti (Alps); 8. Summit (Greenland); 9. ACT2 (Greenland); 10. Devon Island (Canadian High Arctic). Right: inset of the TP region showing the different ice core sites.

## 1. Introduction

Anthropogenic emissions (e.g., greenhouse gases, trace elements) to the atmosphere have dramatically increased since the Industrial Revolution in the 19th century. Trace elements (TEs) are emitted to the atmosphere from both natural sources including wind-borne dust particles, sea salt, volcanoes, forest fires and biogenic emissions (Nriagu, 1989a) and anthropogenic processes such as fossil fuel combustion, mining, ferrous and non-ferrous metal production, and waste incineration (Pacyna and Pacyna, 2001; Marx and McGowan, 2010). It was estimated that during the mid-1990s fossil fuel combustion (primarily coal and oil) was the dominant source of atmospheric TEs worldwide followed by metal production processes and mining (Pacyna and Pacyna, 2001; Marx and McGowan, 2010). Currently, coal, oil, and natural gas, are still the primary sources of global energy (BP, 2016). Coal has been an important fossil fuel since the onset of the Industrial Revolution and is expected to continue in wide use due to its abundant reserves around the world (Shafiee and Topal, 2009; BP, 2016).

High temperature processes such as fossil fuel combustion and pyrometallurgy generate fumes and fine particles ($< 0.1$ μm–10 μm) containing toxic metals (e.g., Cd, Zn, Pb) (Sobanska et al., 1999; Ohmsen, 2001) that if not captured by emission controls can have an atmospheric residence time of ~10 days, giving them sufficient time to be transported over long distances and subsequently deposited far from their emission sources (Quinn and Ondov, 1998; Pacyna and Pacyna, 2001; Marx and McGowan, 2010). Trace elements can have adverse effects on humans and other terrestrial and aquatic organisms depending on their toxicity and bioavailability (e.g., physical and chemical form).

Atmospheric TE monitoring programs, along with emission inventories, have been conducted in recent decades (Nriagu, 1989a; Olendrzynski et al., 1996; Pacyna and Pacyna, 2001; Tian et al., 2015). However, they lack pre-1900 information which is necessary to contextualize current atmospheric changes. Natural archives that receive only atmospheric input and that are geomorphically stable such as lake sediments, peat bogs and ice cores are best to reconstruct records of past atmospheric metal depositions (Cooke and Bindler, 2015; Gabrielli and Vallelonga, 2015; Hansson et al., 2015; Marx et al., 2016). These archives provide different advantages/disadvantages as explained below.

Lakes and ombrotrophic peat bogs are widespread around the world whereas ice fields are confined to polar and high altitude regions. Lakes and peat bogs are easier to access and sample. Because of their location, lake sediments and peat bogs provide local/regional information allowing the study of small and medium scale variability while glaciers receive long-range inputs recording large-scale variability. Glaciers are fed exclusively by atmospheric inputs which is a great advantage to study atmospheric metal depositions compared to peat bogs and lake sediments which can be subjected to both atmospheric and terrestrial inputs. Peat bogs, as opposed to ice cores, are dated based on indirect methods such as $^{14}C$, decreasing their chronology precision. Other than TEs, several additional parameters (e.g., dust particles concentrations, soluble ions concentrations) can be measured in ice cores in co-registered samples to have a better understanding of the possible sources. Moreover, much higher temporal resolution can be achieved in ice cores (seasonal/annual) compared to peat bogs (decadal to centennial) and to lake sediments (decadal/centennial to millennial) (Shotyk, 1996; Shotyk et al., 1998; Martínez Cortizas et al., 2002; Kylander et al., 2010; Ferrat et al., 2012; Bradley, 2015; Cooke and Bindler, 2015; Gabrielli and Vallelonga, 2015; Hansson et al., 2015; Shotyk et al., 2017) making ice cores an extremely useful tool to study past atmospheric pollution.

Glaciers and ice sheets preserve atmospheric species that are deposited as snow accumulates over time, thus creating valuable records of past climatic/environmental conditions. Glaciers act as sinks of atmospheric species, but they can also serve as sources by releasing TEs in meltwater (Zhang et al., 2015a) which may affect the people who depend on glacial meltwater. Ice cores from polar glaciers and ice sheets have been used to obtain TE records. However, only a few non-polar ice core records (Hong et al., 2009; Kaspari et al., 2009; Lee et al., 2011; Eichler et al., 2014; Gabrielli et al., 2014; Uglietti et al., 2015; Wang et al., 2016; Beaudon et al., 2017) provide continuous information back to pre-industrial times. Thus, ice core records of TEs from mid- and low-latitudes are needed to assess the spatial and temporal extent and levels of pollution in the environment. This information can be used by modelers to assess pollution transport at local, regional, and global scales and by policy makers to develop strategies and policies to reduce their emissions.

The Tibetan Plateau (TP) comprises ~46,000 glaciers in an area of ~100,000 km$^2$ (Yao et al., 2012). These glaciers collectively contain the largest natural reservoir of ice outside of the Polar Regions and are the primary source for major rivers in Asia. The Guliya ice cap (35°17′N, 81°29′E; 6200 m asl) located in the western Kunlun Mountains on the Qinghai-Tibetan Plateau, China (Fig. 1), is the largest ($> 200$ km$^2$) ice cap in the subtropical zone. Guliya resembles a “polar” ice cap with low temperatures and low precipitation (Thompson et al., 1995, 1997).

The atmospheric circulation over the TP is controlled by the East Asian and South Asian summer monsoons, the westerlies that ultimately originate over the North Atlantic, and their interactions (Schiemann et al., 2009; Yao et al., 2013; Maussion et al., 2014). The pronounced seasonality on the TP affects the intensity and position of the westerly jet. During winter (December–February), the westerlies are strong and dominate over the TP as the result of a geopotential height

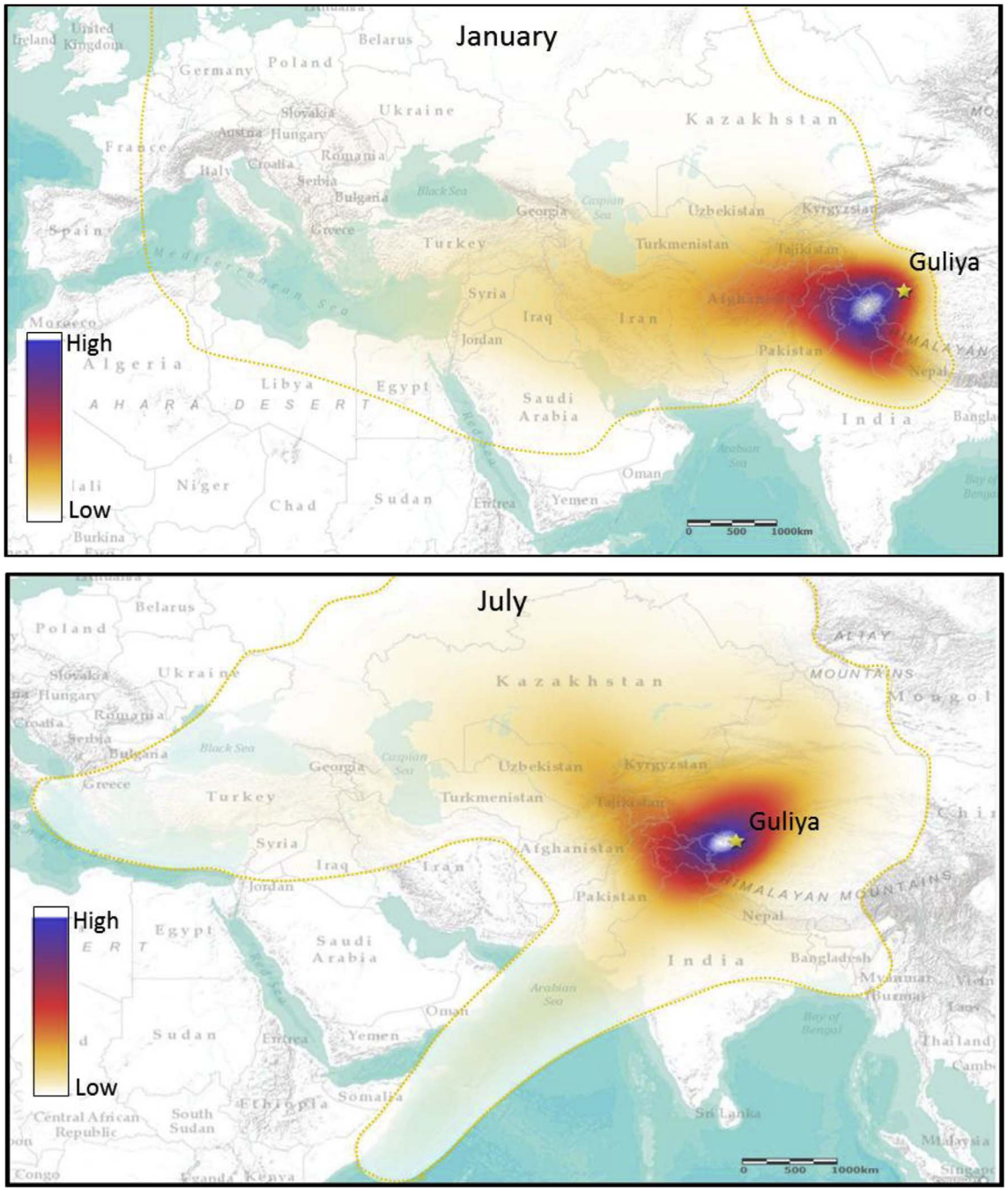


**Fig. 2.** NOAA HYSPLIT 7-day back trajectories frequency plots for every day of January (middle of the dry season) and of July (middle of the wet season) using NCEP Reanalysis 1 for the 1948–1992 period (Stein et al., 2015; Rolph et al., 2017). Frequencies are shown by areas shaded from white and dark blue (high frequency) to orange and yellow (low frequency). (For interpretation of the references to color in this figure legend, the reader is referred to the Web version of this article.)

gradient in the region. The TP is mostly dry during the winter season (Tian et al., 2007; Schiemann et al., 2009; Maussion et al., 2014). In summer (June–August) the monsoon changes the atmospheric circulation over the TP. The westerlies weaken and their main axis shifts to the north ~40–42°N (Schiemann et al., 2009; Maussion et al., 2014), whereas the northern limit of the monsoon reaches ~34–35°N (Tian et al., 2007). The westerly flow splits during summer into a north and south branch due to the topography and the Tibetan low. Guliya, located at 35°17′N, is dominated by the westerlies during winter while during summer it experiences a combination of southerly (monsoonal) and westerly flows due to the shift of the westerly jet to the north and the monsoon onset (Fig. 2). Guliya receives most of its precipitation (~80%) during spring (March–May) and summer, and the rest during winter (Schiemann et al., 2009; Maussion et al., 2014). The precipitation over Guliya seems to result from continental water recycling through convective activity (Numaguti, 1999; Tian et al., 2001; Maussion et al., 2014). Because of its continental location on the northwestern side of the Tibetan Plateau and the dominance of the westerlies, the Guliya ice cap is expected to be unaffected by the fallout of anthropogenic trace metals originating from inner Asia (eastern China) but to record trace metal emissions from western countries.

Trace element ice core records from the Himalayas and Tibet have shown regional anthropogenic inputs mainly during the second half of the 20th century. Increases of Pb, As, Mo, Sn, Sb, Bi, U, and Cs in Mt. Everest since ~1970s were attributed to fossil fuel combustion from India and Nepal (Hong et al., 2009; Kaspari et al., 2009; Lee et al.,

2011). The Belukha glacier in the Altai region shows increases of Cd, Cu, Sb, Zn, and Pb between 1935 and 1980 CE (Common Era; henceforth all dates are in CE) from non-ferrous metal production and fossil fuel combustion from the Soviet Union (SU) (Eichler et al., 2012, 2014). Anthropogenic emissions (e.g., non-ferrous metal production and fossil fuel combustion) from Central Asia and western China were observed in ice core records from Inilchek in Central Tien Shan (Grigholm et al., 2016), Miaoergou in the eastern Tien Shan (Liu et al., 2011; Wang et al., 2016), and Muztagh Ata in the Eastern Pamirs (Li et al., 2006) as increases of Pb, Cd, Cu, Sb, Bi, Tl, and Sn after 1950s. And more recently, anthropogenic emissions from the SU between 1930 and 1980s as well as recent pollution depositions from India and China were detected in Puruogangri, Central Tibet, (Beaudon et al., 2017). Also in Central Tibet, a ~1500–1990 ice core-derived Hg record from Mt. Geladaindong shows an increase since the Industrial Revolution to 1982 (top of the record) reflecting recent pollution from South Asia (Kang et al., 2016). These Himalayan/Tibetan ice core records have greatly contributed to study pollution in the region. However, only a few of them (Belukha, Mt. Everest, Puruogangri and Geladaindong) cover at least part of the pre-industrial period, which is essential to assess pollution trends that extend beyond modern instrumental records and emission inventories. This leaves an important geographical gap in the Northwestern TP that the Guliya TE ice core record can bridge.

Here we present TEs records (concentration, enrichment factor (EF), and excess (Ex) concentration) spanning the period 1650–1991 from the Guliya ice core to assess their natural and anthropogenic sources throughout this period. The Guliya TEs records are the only records from the Northwestern TP that cover the pre-industrial period, thus filling a critical geographical and temporal gap in the investigation of atmospheric emissions sources and their geographical origin both before and after the Industrial Revolution.

## 2. Methods

### 2.1. Ice core

Three ice cores (93.2, 308.6, and 34.5 m) were recovered from the Guliya ice cap (35°17′N, 81°29′E; 6200 m asl; Fig. 1) in 1992 as part of an American-Chinese expedition. Details of the drilling operation can be found in Thompson et al. (1995). The mean accumulation rate at the site is ~0.2 m water equivalent per year (Thompson et al., 1995, 1997). The timescale in this study is based on annual dust layer counting (Thompson et al., 1995, 2006a; Davis, 2002) and is constrained at 5.4 m to the year 1963 where the beta radioactivity rose above the natural background in response to thermonuclear tests by the former SU.

### 2.2. Sample preparation and analysis

#### 2.2.1. Ice samples

The TE analysis of the Guliya ice core was performed continuously from the depth of 0.96 m (corresponding to the year of 1991) to 59.33 m (corresponding to the year of 1645) from Core 2 (308.6 m). The top 0.96 m consisted of firn and there was not enough material (mass) to be processed. A total of 1348 ice samples were cut with a band saw in a cold room at −5 °C. The sample length varied from 2.5 cm to 16 cm (Figure A1a) depending on the resolution needed and the ice mass available. Ice core sampling was sub-annually resolved from 1750 to 1991 and annually/multi-annually resolved from 1645 to 1750 (Figure A1b). Samples were decontaminated in a class 100 clean room by triple rinsing with ultrapure water (18.3 MΩ) (Gabrielli et al., 2014; Uglietti et al., 2014, 2015). The samples were melted at room temperature in acid pre-cleaned (Candelone et al., 1994; Gabrielli et al., 2014) low-density polyethylene (LDPE) bottles (Nalgene) then transferred to acid pre-cleaned LDPE vials and acidified with optima grade $HNO_3$ (Fisher Scientific) to obtain a final concentration of $HNO_3$ 2% (v/v). The acidified samples were kept in a class 100 clean room for 30 days to allow the acid to leach the TEs. Samples were then analyzed or frozen until analysis (Uglietti et al., 2014, 2015).

The samples were analyzed by Inductively Coupled Plasma Sector Field Mass Spectrometry (ICP-SFMS) (Element 2, Thermo Finnigan) coupled with a desolvation introduction system (Apex Q, ESI) (Uglietti et al., 2014). Twenty-nine TEs were determined: Ag, Al, As, Ba, Bi, Cd, Co, Cr, Cs, Cu, Fe, Ga, Li, Mg, Mn, Mo, Na, Nb, Ni, Pb, Rb, Sb, Sn, Sr, Ti, Tl, U, V, and Zn.

External calibrations were performed at the beginning and end of the analytical session as well as in the middle of the session when more than 30 samples were analyzed. Procedural blanks were prepared as described by Uglietti et al. (2014) to determine any possible contamination during the sample preparation. Procedural blanks were below 2% of the median concentration for all TEs (except Nb (9%)) and thus were negligible. Limits of detection were determined as 3 times the standard deviation of 10 measurements of a blank (optima $HNO_3$ 2% ultrapure water solution) and ranged from 0.01 pg/g for Ag, Cd, Sb, Cs, and Bi to 204 pg/g for Fe and 361 pg/g for Na, which are in agreement with those previously obtained (Gabrielli et al., 2014; Uglietti et al., 2014; Beaudon et al., 2017).

ICP-SFMS accuracy was assessed every day of analysis using a certified material solution (TMRain-95, Environment Canada), which was diluted by a factor of ~20. The concentrations measured were within the uncertainty range of the certified concentrations. The instrument precision was measured by re-analyzing 16 different Guliya ice samples several months after the first analysis. The precision ranged within 4–10% for all TEs except Nb and Sn (17%), and Ag (22%).

#### 2.2.2. Potential source area (PSA) samples

Dust samples collected from 8 different sites during 1992 and 2015 in the vicinity of the Guliya ice cap were used to represent the potential source area (PSA) of the TEs deposited on the ice cap (Figure A2). PSA samples were prepared by adding between 0.1 g and 0.5 g of dust to a 250-ml acid pre-cleaned LDPE bottle containing ultrapure water. Before adding the dust to the ultrapure water, three aliquots of 10 ml of ultrapure water were transferred from the 250-ml bottles into three acid pre-cleaned LDPE vials and used as procedural blanks. After adding the dust, the bottles were shaken and let sit for 2 min to allow the large particles to settle. The supernatant solution, containing particles with a size comparable to that of aeolian dust entrapped in the ice, was sampled by pipetting three aliquots of ~10 ml into three acid pre-cleaned LDPE vials. Procedural blanks and samples were prepared and analyzed by ICP-SFMS similarly to the ice samples. The TE concentrations of the procedural blank replicates were averaged and subtracted from each PSA sample before obtaining the final PSA average.

### 2.3. Enrichment factor (EF) and potential source area (PSA)

To determine whether the TE concentrations measured are of crustal or non-crustal origin, EFs and Ex concentrations were calculated. EFs were obtained from the equation $EF = [TE/Fe]_{ice}/[TE/Fe]_{PSA}$ where is the TE mass ratio in the ice sample using Fe as a crustal element and $[TE/Fe]_{PSA}$ is the corresponding ratio in the Guliya PSA. The EF absolute values depend on the crustal TE used as a reference (e.g., Fe, Al, Ba) and on the crustal reference adopted (e.g., upper continental crust (UCC), PSA) (Krachler et al., 2005; Marx et al., 2016).

Fe is used here as a crustal element because (1) it is the crustal element with the highest abundance in the Guliya PSA and in the Guliya ice samples; (2) Fe concentrations are relatively stable and abundant (6% (Wedepohl, 1995)) in rocks and soil; and (3) it is determined with high precision (6%) and accuracy (3%) (Uglietti et al., 2014). A multivariate analysis of TE concentrations (Table A1) confirms that Fe, Al, Mg, and Ba are of crustal origin. Fe is highly correlated with Al ($r = 0.98$), Mg ($r = 0.98$), and Ba ($r = 0.94$) and the EFs of Al (Fig. 3), Mg, and Ba are constant (close to 1) throughout the period studied here.

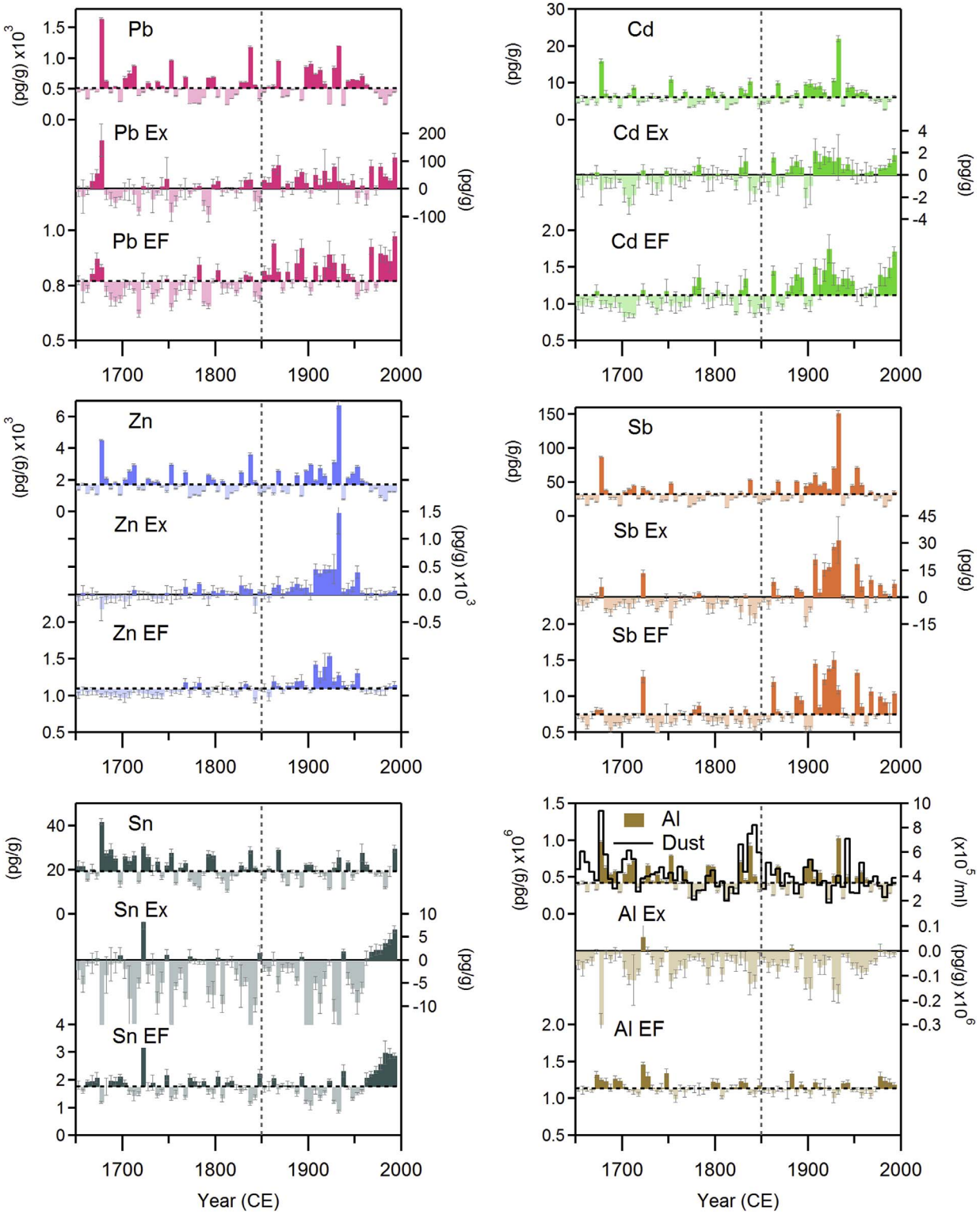


**Fig. 3.** Five-year median concentrations and instrumental standard deviation, excess (Ex) concentrations, and enrichment factors (EF) including propagated uncertainty (Miller and Miller, 2010) of Pb, Cd, Zn, Sb, Sn, and Al between 1650 and 1991. Dust particle concentrations (solid line) for particles 0.63–20 μm (Thompson et al., 1997) are shown in the Al top panel for comparison. The horizontal dotted lines show the 1650–1991 concentration (top panels) and EF medians (bottom panels). The vertical dotted line marks the onset of Pb, Cd, Zn, and Sb enrichment observed post-1850s.

The EFs of the Guliya ice samples were also determined using Al, Mg, and Ba as crustal elements and no significant differences were observed. Thus, using Fe as a crustal element to calculate EFs does not influence our results.

The TE mean composition of the UCC (Wedepohl, 1995) is often used to calculate EFs. However, there are some uncertainties associated with its use. First, the UCC concentrations were obtained by X-ray fluorescence spectrometry and atomic absorption spectroscopy (Shaw et al., 1967, 1976) providing total elemental concentrations while the 2% acidification used in this study releases only a fraction of the total

TEs in the sample (Uglietti et al., 2014). Second, a large variability may be introduced when using the UCC due to differences in chemical composition from the local dust.

The geochemical composition of the TP dust is characteristic of this region (Li et al., 2009) when compared with the average terrestrial dust composition (UCC) and within the TP (Wu et al., 2009a, 2009b). Li et al. (2009) found that TP soils are enriched in As, Cs, and Bi relative to the UCC especially in the aeolian-like fraction (< 20 μm). Wu et al., (2009a) determined that Ca/Al and Fe/Al rations from dust aerosol samples at Muztagata (4430 m asl) in the Eastern Pamirs were distinct from Central Tibet (Inilchek). Thus, adopting the PSA (aeolian fraction) as a reference and preparing it similarly to the ice core samples reduces the uncertainties associated with the use of the UCC and eliminates analytical uncertainties.

When using UCC as a reference, an EF threshold of 10 is commonly used to discriminate between crustal and non-crustal sources (Zoller et al., 1974; Duce et al., 1975). When using the local dust as a reference, an arbitrary EF threshold (e.g., 10) is no longer required (Krachler et al., 2005; Hong et al., 2009; Uglietti et al., 2015; Marx et al., 2016; Beaudon et al., 2017).

EFs calculated relative to the PSA from non-crustal contributions are much smaller than those obtained using the UCC (Krachler et al., 2005; Hong et al., 2009; Uglietti et al., 2015; Beaudon et al., 2017) since the PSA TE composition is a close representation of the background crustal composition in the ice. As an example, the Sb EF is used here to demonstrate some of the differences between using UCC and local dust as references. The Sb $EF_{UCC}$ and the $EF_{PSA}$ in a sample from ~1933 is ~32 and 5 respectively. The former suggests anthropogenic sources and the latter crustal sources if the typical EF threshold of 10 is used. However, the $EF_{PSA}$ is significantly higher than the pre-1850 EF median of 0.7 suggesting anthropogenic sources even though the EF value is < 10. Both Sb EFs ($EF_{UCC}$ and $EF_{PSA}$) increased by a factor of ~7 in that 1933 sample compared with the pre-1850 period. Therefore, to determine if a TE is enriched in a record like the Guliya ice core, it is necessary to have the pre-industrial period (1650–1750 in Guliya) to provide the natural background. A TE can be considered enriched when its EF is significantly higher (Mann-Whitney test: $p < 0.0005$ for medians) than pre-industrial or background levels and when a sustained trend is observed in a record (Marx et al., 2016). While we show these deviations are significant, excess (Ex) concentration of the TEs was used to further corroborate the EF results.

### 2.4. Excess (Ex) concentration

Excess concentrations were obtained using the equation

$$Ex = TE_{ice} - [TE/Fe]_{pre-industrial\ ice} \times [Fe]_{ice}$$

where $[TE/Fe]_{pre\text{-}industrial\ ice}$ corresponds to the median mass ratio of the TE of interest to Fe over the 1650–1750 period (assumed as the pre-industrial background at Guliya).

Thus, two different approaches, using independent standards, are employed to determine if the TE is of crustal or non-crustal origin. In the first approach, the Guliya PSA is used as a crustal reference to obtain the EF, and in the second approach the pre-industrial elemental composition in the Guliya ice core record between 1650 and 1750 is used to determine the Ex concentration. Here, only TEs that display significant increases (per the Mann-Whitney test: $p < 0.0005$) of both EF and Ex concentration are considered enriched. This study focuses on the non-crustal origin of the enriched TEs (Pb, Cd, Zn. Sb, and Sn).

### 2.5. Statistical analysis

A multivariate factor analysis was performed using Minitab 17 on the entire data set of ranked concentrations using the varimax rotation (Gabrielli et al., 2008, 2014). A multivariate Ward hierarchical cluster analysis was applied to the matrix of the first three factors using Euclidean distance to better visualize the association of TEs (Gabrielli et al., 2008, 2014) during the entire period (1650–1991) and during the pre-1850 and post-1850 periods (1850–1950, 1950–1991).

In this analysis and the accompanying graphs, median values are used to avoid outliers (e.g., from possible dust events), which may skew the results. Five-year median concentrations and EF values were calculated using the data comprised within the 5 years before the assigned date. For example, the median value linked to the year 1970 was computed using the values between 1965 and 1969.

## 3. Results and discussion

### 3.1. Natural sources

A statistical summary of concentrations, EFs and Ex concentrations, is presented in Tables A2-A4 for the pre-1850 and the two post-1850 periods (1850–1950; 1950–1991). Concentrations of typical crustal TE covary with dust (Fe: $r = 0.68$, $p < 0.001$; Al: $r = 0.65$, $p < 0.001$) since they are derived mainly from mineral dust (Tables A1, A2). The multivariate analysis of TE concentrations (Table A1) was performed to extract shared variance amongst TEs and to help identify general sources. Three factors were obtained corresponding to 70%, 19%, and 7% of the total variance of the 29 TEs (Table A1). Factor 1 is strongly loaded in crustal elements (Ag, Al, As, Ba, Bi, Co, Cr, Cs, Cu, Fe, Ga, Mg, Mn, Nb, Ni, Rb, Ti, Tl, V, Fe, Tl, and V). Factor 2 is mainly loaded by the evaporite minerals Na (halite, NaCl) and Sr (celestite $SrSO_4$) (Merian et al., 2004). Both Na and Sr have been detected in saline lakes of the Qinghai TP, east of Guliya (Zheng and Liu, 2009), and in snow melt from the Tien Shan mountains (Le Callonnec et al., 2005). Factor 2 is also loaded to a lesser extent in Mo, Li and Ti. Mo is associated with granitic rocks, and its principal mineral molybdenite ($MoS_2$) is associated with Fe and Ti (Merian et al., 2004) explaining the relatively high load of Ti in Factor 2. Li is a typical evaporite in saline lakes of the TP (Zheng and Liu, 2009). The Amu Darya river, fed by the Pamirs meltwater flows northwest to the Aral Sea, passes along Afghanistan, which is rich in mineral deposits such as Mo and Li and minerals like calcite, gypsum, celestite, and evaporites (Kokaly et al., 2011; Stone, 2014). The river discharges dissolved TEs such as Mo that can become evaporatively enriched in aquatic systems forming oxy-anions (Schettler et al., 2013). Thus, Mo in the form of evaporite oxy-anion may reach Guliya along with other evaporite elements such as Na and Sr. Factor 3 is loaded by Cd, Sb, and Zn suggesting their anthropogenic origin as discussed in Section 3.2.

The Guliya dust concentrations are among the highest in the TP ranging between $4.5 \times 10^4$ and $1 \times 10^8$ particles/ml with a median of $3.8 \times 10^5$ and an average of $1 \times 10^6$ particles (0.63–20 μm diameter)/ml (Fig. 3) between 1650 and 1991 (Thompson et al., 1995; Davis, 2002). Thus, TE concentrations are very large. For example, Al (Fig. 3) and Fe concentrations range between 0.03 μg/g to 6 and 11 μg/g, respectively (Table A2).

Fig. 3 shows 5-year median concentration time series of Pb, Cd, Zn, Sb, Sn, and Al. Fig. 3 and Table A2 show that post-1850 concentrations of Pb, Cd, Zn, and Sb are higher than the pre-1850 concentrations. The median concentrations during the 1850–1950 period increased by 30% (Sb), 20% (Cd and Zn), and 10% (Pb) (Table A2).

Dust is the most abundant aerosol around the TP (Kuhlmann and Quaas, 2010) with local and remote deserts as its main sources (Sun et al., 2001; Zhang et al., 2001; Wu et al., 2009a, 2009b). Zhang et al. (1996) determined that ~70% of the aerosol dust particles in Tibet is from local dust sources with the rest originating from distant sources. Wu et al. (2009a) determined that the rare earth elements compositions of the dust entrapped in an ice core from Muztagata glacier (6250 m asl) and that of aerosols collected just below the glacier (4430 m asl) are similar suggesting common provenance. In the case of Guliya, the TE composition of the ice core samples was compared with that of the Guliya PSAs. The $EF_{UCC}$ for all eight PSA samples show enrichment in

As and Bi (Figure A3) in agreement with Li et al. (2009). In addition to As and Bi, we found that Sb is also enriched in the Guliya PSAs (Figure A3-A4). An $EF_{UCC}$ average of the eight PSAs was determined for all TEs and compared to the TE $EF_{UCC}$ medians of the Guliya ice calculated over the entire record (Figure A4). All Guliya ice $EF_{UCC}$ values for all TEs are comparable to those of the PSA suggesting the main source of dust deposited on Guliya likely originates from the soils around the ice cap, supporting the use of the Guliya PSA to discriminate non-crustal sources.

The TEs concentrations in Guliya decrease after ~1960 (Fig. 3). This decrease in concentration is likely associated with a decline in dust input as observed in other studies. For instance, a decrease in dust/TEs was observed in the Geladaindong ice core (Grigholm et al., 2015; Zhang et al., 2015b) and the Puruogangri ice core (Thompson et al., 2006b; Beaudon et al., 2017) from Central Tibet. The decrease in dust input can be the result of a reduction in the frequency of dust storms after the 1960s - 1970s such as those detected in central Asia (Indoitu et al., 2012), northern China (Qian et al., 2002), and northwest China (Zhao et al., 2013).

### 3.2. Anthropogenic sources

As stated above, two approaches (EF and Ex concentrations) are used in this study to determine if a TE is enriched (of non-crustal origin) in the dust-laden Guliya ice core. Despite the disadvantageous high dust concentrations to discern crustal from non-crustal sources, significant enrichments for Cd, Sb, Sn, Pb, and Zn were observed at different times during the post-1850 period (Fig. 3).

The EF and Ex concentrations of Pb, Cd, Zn, Sb, and Sn in Guliya are shown in Fig. 3. The EFs and Ex concentrations for all TEs for the periods studied here are presented in Appendix A (Table A3, A4). Enrichment of these five TEs occurs during all (Pb, Cd, and Sb) or some part (Zn and Sn) of the 1850 to 1991 period, yielding different temporal patterns. Pb, Cd, and Sb (Sb to a lesser extent) are enriched over the entire period while Zn is enriched primarily from 1900 to 1950 and Sn enrichment is restricted almost exclusively to the post-1950 interval.

To investigate the possible anthropogenic emission sources of the observed TEs enrichments during the late 19th and the 20th centuries, the Guliya TE records are compared with other ice core records as well as production, consumption, and/or information from emission databases and inventories. For a homogenous comparison, the EFs of the different records (including Guliya) are standardized and presented as z-scores.

#### 3.2.1. Pb, Cd, Zn, and Sb from coal combustion (~1850–1950)

Coal combustion fly ash is enriched in TEs such as Cd, Sb, Pb, and Zn among others (Xu et al., 2004; Reddy et al., 2005). For example, Pacyna and Pacyna (2001) estimated that during the mid-1990s, coal combustion was the largest single source of anthropogenic Sb (~50% of total Sb emissions), the second major source of Cd and Zn, and the third major source of Pb (leaded gasoline being its main source during the 1990s) worldwide. The multivariate factor analysis (Table A1) and cluster analysis of TEs during the periods studied here suggest that Zn is linked to Cd and Sb during the 1850–1950 period (Figure A5). In coal combustion fly ashes, Cd, Sb, and Zn are associated primarily with the coal sulfide fraction possibly explaining their linkage in the cluster analysis. In contrast, Pb in coal is usually associated with the clay minerals and feldspar fraction and therefore it does not cluster with Zn, Cd, or Sb (Xu et al., 2004). Therefore, synchronous depositions of Cd, Sb, Pb, and Zn are likely linked to coal combustion, especially before the widespread use of oil (~1950) and the largest consumption of leaded gasoline (~1950s-1980s).

A comparison of the Guliya Pb EF z-scores with other ice cores at regional and Northern Hemispheric scales is shown in Fig. 4. Pb is used for this comparison since it is one of the most studied TEs and several Pb records exist from different regions. Tibetan (Li et al., 2006; Liu et al., 2011; Eichler et al., 2012, 2014; Grigholm et al., 2016; Wang et al., 2016; Beaudon et al., 2017) and Himalayan (Hong et al., 2009; Kaspari et al., 2009; Lee et al., 2011) ice core records show regional anthropogenic inputs mainly since the second half of the 20th century (Fig. 4A). Likewise, lake sediments (Jin et al., 2010; Wang et al., 2010) and peat bogs (Bao et al., 2010, 2015) from North Eastern Tibet have recorded rapid increases of TEs after 1960/1970 concomitant with the exponential economic development in China and India and their use of coal (BP, 2016). In contrast, ice core records from Devon Island (Krachler et al., 2005; Shotyk et al., 2005) in the Canadian Arctic; ACT2 (McConnell and Edwards, 2008) and Summit (Candelone et al., 1995; McConnell et al., 2002) in Greenland (not shown) and Colle Gnifetti in

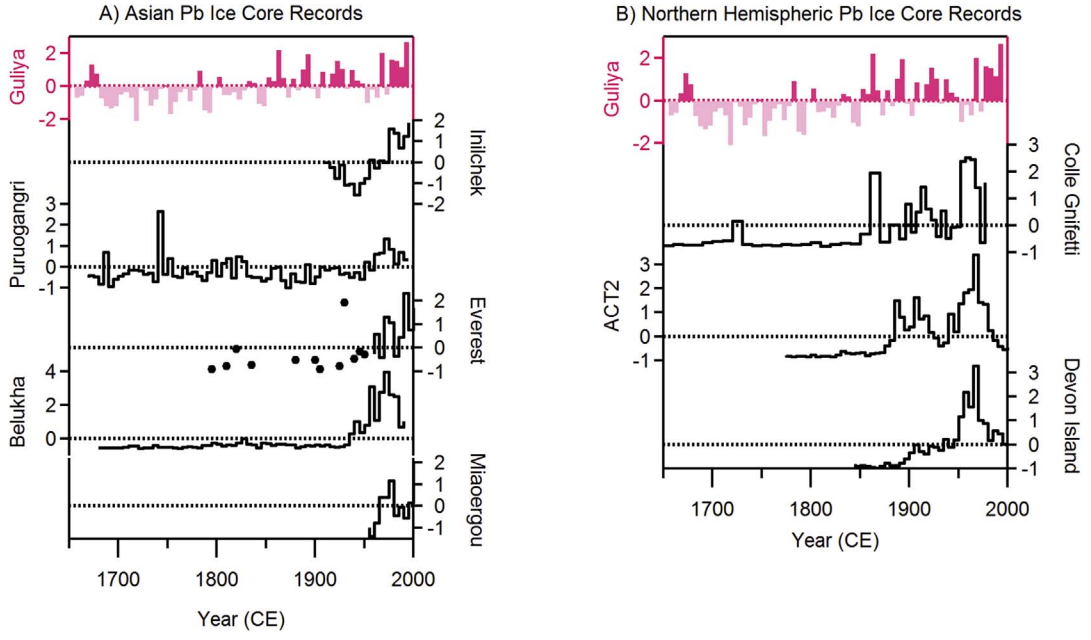


**Fig. 4.** Guliya Pb EF z-scores compared on regional and hemispheric scales. A) Regional scale includes ice cores from Inilchek (Grigholm et al., 2016); Puruogangri (Beaudon et al., 2017); Everest (Lee et al., 2011); Belukha (Eichler et al., 2014); and Miaoergou (Liu et al., 2011). B) Hemispheric scale includes ice core records from: Colle Gnifetti (Schwikowski et al., 2004), ACT2 (McConnell and Edwards, 2008), and Devon Island (Shotyk et al., 2005). All data are five-year medians except Everest (1650–1960) which is displayed at sample resolution.

the European Alps (Barbante et al., 2004; Schwikowski et al., 2004) show TE increases between the late 1800s to early 1900s (Fig. 4B). On Devon Island, the post-1900 increase of Pb and Sb EFs was attributed to coal combustion and mining and smelting of Pb and Cu ores mostly in Eurasia (Krachler et al., 2005; Shotyk et al., 2005). Increases of Pb and Cd in the ACT2 ice core record correlate with black carbon measurements between ~1887 and ~1948 and therefore were attributed to coal combustion in Europe and North America (McConnell and Edwards, 2008). In the Colle Gnifetti core, Pb concentrations and EFs (Schwikowski et al., 2004), and Zn concentrations (Barbante et al., 2004) increased above the pre-1860s background between 1860 and 1930. Pb increases in Colle Gnifetti during this period were associated mainly with coal combustion in Europe due to the concomitant increases of black carbon observed in the ice core (Lavanchy et al., 1999; Schwikowski et al., 2004). Additionally, Pb increases observed during the 1800s in peat bog records from Europe (Shotyk et al., 1998; Weiss et al., 1999; Martínez Cortizas et al., 2012) were associated with the onset of the Industrial Revolution.

Pb enrichments are observed in Guliya after the 1850s similar to Colle Gnifetti, ACT2 and Devon Island. Marx et al. (2016) compiled Pb records from lakes, peat mires, and ice cores from around the world and determined that Pb, along with other metals, became globally ubiquitous after ~1850 leaving a fingerprint even in sedimentary records with a small atmospheric contribution. The TEs enrichments observed after the 1850s reflect the long-range transport of metals due to the significant worldwide pollution increase that accompanied the onset of the Industrial Revolution (i.e., ~1840 to 1870).

Coal/oil production from the "Organisation for Economic Cooperation and Development" European countries (OECD Europe) and North America (HYDE, 2006a), as well as coal/oil consumption from Europe, SU, Russia, Commonwealth of Independent States (CIS), China, India, and North America (BP, 2016) are compared with a Guliya Pb-Cd-Zn-Sb EF composite (Fig. 5). Coal production in OECD Europe and North America increased since the Industrial Revolution at the end of the 19th century reaching its maximum between ~1905 and ~1960. In Europe, coal production decreased after 1960 due to the shift to oil and

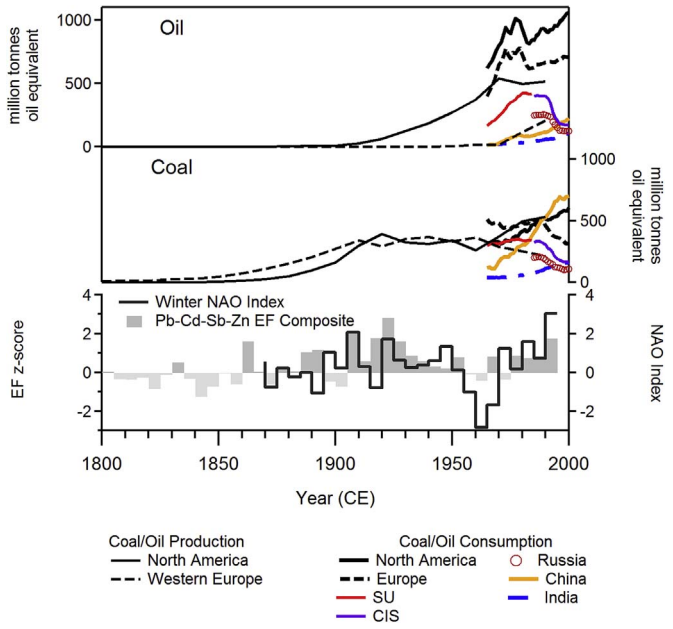


**Fig. 5.** Comparisons of Pb-Cd-Zn-Sb EFs composite (average of Pb, Cd, Zn, and Sb EF z-scores) with coal/oil production (HYDE, 2006a) in North America and Western Europe, and coal/oil consumption (BP, 2016) from North America, Europe, Soviet Union (SU), Commonwealth of Independent States (CIS), Russia, China and India. EF z-scores shown as five-year medians. The winter (December through March) NAO index is shown in the bottom panel as 5-year medians (Hurrell, 2003). (For interpretation of the references to colour in this figure legend, the reader is referred to the Web version of this article.)

natural gas consumption (Pacyna and Pacyna, 2001; Novakov et al., 2003; Bond et al., 2007) whereas in North America the production and consumption of coal has continued to increase. The coal consumption in the SU and/or CIS peaked during the second half of the 20th century (~1980s) and decreased in the 1990s corresponding to the SU economic decline (BP, 2016). More recently, China and India have increased their coal consumption since 1970. The Guliya Pb-Cd-Zn-Sb EF composite trend coincides with coal production from OECD Europe and North America during the second half of the 19th century and the first half of the 20th century. Combining the observations of the deposition and emission records we suggest that, while emissions from North America are unlikely to have reached the Guliya ice cap, European coal combustion emissions are likely the main source of the observed Pb, Cd, Sb, and Zn enrichments. Future Pb isotope and black carbon measurements could potentially lend support for this conclusion.

A 7-day NOAA HYSPLIT back-trajectory frequency analysis was performed over the 1948–1992 period for every day of January (middle of the dry season) and July (middle of the wet season) to geographically constrain the atmospheric influence at the Guliya ice cap. The back-trajectory frequency analysis (Fig. 2) shows that, as described in the introduction, Guliya is dominated by westerlies during the winter. The area of influence during winter comprises Central Asia (Kyrgyzstan, Tajikistan, Afghanistan, Pakistan, Uzbekistan, Turkmenistan), Northwestern India, the Middle East, Northern Africa, Eastern, and Western Europe. The highest density of back trajectories covers only Central Asia whereas the lowest density extends to Western Europe and North America. In summer, the area of influence is smaller compared to winter. Air masses from Kyrgyzstan, Tajikistan, western China (Xinjian province), Uzbekistan and Kazakhstan dominate the back trajectories. Air masses from South Asia (e.g., India, Nepal, and Bangladesh) can also reach Guliya due to the Indian monsoon influence in summer. During 1850–1950, North America and Europe were the main coal combustion emitters. The Guliya winter back trajectories extend to Europe during 1948–1991 and this is likely to have been the case from 1850 to 1948. Thus, Europe, one of the two main polluters at the time, is very likely the primary source of TE enrichment observed in the Guliya ice core.

### 3.2.2. Sn, Cd, and Pb enrichments (Post-1950s)

Enrichments of Sn (20%), Cd (20%), and Pb (10%) were observed during the post-1950s (Table A3). Sn enrichment is detected since 1965 while Cd and Pb enrichments are observed starting in 1975 (Fig. 3). Sn EF increased significantly by 60% during 1965–1991 relative to the pre-1850 period. Cd and Pb EFs increased significantly by 40% and 20% respectively during 1975–1991 compared to the pre-1850 period.

*3.2.2.1. Sn.* A comparison of Sn EF z-scores in Guliya with the Miaoergou and Everest ice cores shows increases of Sn in Miaoergou (Liu et al., 2011) after the 1950s and in Everest (Hong et al., 2009) after 1970 (Fig. 6). These Sn increases were attributed to stationary fossil fuel combustion and non-ferrous metal production from western China and India, respectively. Guliya is primarily affected by westerlies; however, during summer it experiences a combination of southerly and westerly flows (Schiemann et al., 2009; Maussion et al., 2014). Thus, air masses from India/Nepal could reach Guliya and thereby transport pollutants from these regions (Fig. 2).

The observed Sn enrichment since 1965 could have originated from petroleum coke (petcoke) combustion from the OECD European countries and/or from fossil fuel combustion in India and/or western China. In fact, oil combustion, and more specifically petcoke combustion, emits more Sn, relative to other TEs (Sb, Cd, Zn), than coal combustion (Nriagu, 1989b). The OECD Europe shifted from coal to oil combustion ~1960 while countries like the USA, China and India have increased their coal consumption since ~1970 (Fig. 4).

The History Database of the Global Environment (HYDE) (HYDE, 2006b) shows that Sn mining and smelting production (Fig. 5) in the

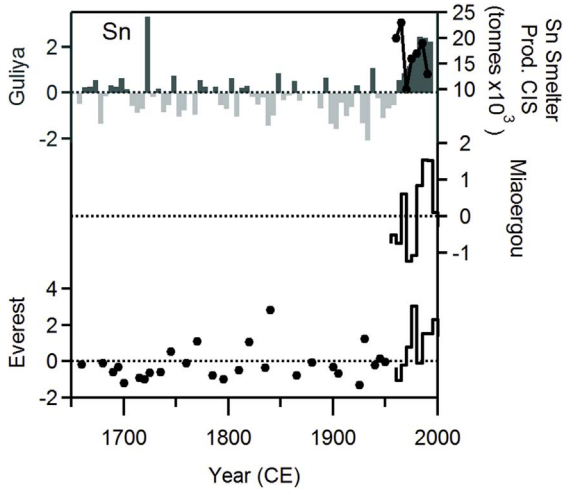


**Fig. 6.** Sn EF z-scores comparison between the Guliya ice core record and ice core records from Miaoergou (Liu et al., 2011) and Everest (Hong et al., 2009). Guliya Sn EF z-score is compared with Sn smelter production (dotted curve) from CIS (HYDE, 2006b) in the top panel.

CIS countries has gradually increased between 1970 and 1985 whereas Sn smelting from OECD European countries has decreased since 1960 by ~60% (HYDE, 2006b). The CIS Sn mining and smelting are also likely sources of Sn to Guliya as they are located upwind of the ice cap.

*3.2.2.2. Cd and Pb*. Current Asian emissions (1970s onwards) have been recorded in different natural archives (ice cores, lake sediments and peat bogs) in the region (Hong et al., 2009; Kaspari et al., 2009; Bao et al., 2010; Jin et al., 2010; Wang et al., 2010; Yang et al., 2010; Lee et al., 2011; Liu et al., 2011; Bao et al., 2015; Grigholm et al., 2016; Kang et al., 2016; Wang et al., 2016; Beaudon et al., 2017). Black carbon from coal combustion in western China was detected in 2012–2014 snow pits from Laohuguo glacier (northern TP) (Li et al., 2016) further showing that recent coal combustion emissions from western China are being captured by glaciers. Thus the 1975–1991 enrichments of Pb and Cd in Guliya could be the result of regional emissions as opposed to the 1850–1950 TEs increases.

The main emission sources of Cd and Pb include fossil fuel combustion and non-ferrous metal production (e.g., Zn, Cu, and Pb). The former has been their main emission source since 1975 in Europe although emissions have been decreasing progressively (Pacyna et al., 2009). The main source of Pb worldwide and in Europe since the 1950s has been the combustion of leaded gasoline, reaching a maximum between 1965 and 1975 and decreasing after 1975 with its progressive phase out (Pacyna and Pacyna, 2001; Pacyna et al., 2009). Non-ferrous metallurgy (e.g., Pb consumption, mining and smelting) reached a maximum in 1980 and then started decreasing along with oil consumption with the SU economic decline (Fig. 7) (HYDE, 2006b; Pacyna et al., 2009), thus, TE emissions decreased simultaneously. As the Guliya Cd and Pb enrichments rise above the median after the European/CIS non-ferrous metallurgy declines (Fig. 7), this suggests different emission sources.

Phosphate fertilizers are important emission sources of Cd, Cu, Pb, and Ni (Nriagu and Pacyna, 1988; Nriagu, 1989b). Grigholm et al. (2016) suggested that the Inilchek glacier may be influenced by phosphate fertilizer emissions from the CIS. Heavy metals such as Cd and Pb are impurities in fertilizers derived from phosphate rocks. Phosphate fertilizer usage increased in the CIS since 1960 (Fig. 8) (FAO, 2016). The Aral Sea desiccation is considered one of the greatest environmental disasters of the 20th century and may yield another source of Cd and Pb for Guliya. In the 1960s, the SU diverted the Amu Darya and Syr Darya rivers to irrigate cotton and rice fields, causing a ~60% decrease in area of the Aral Sea by 1998. Large amounts of fertilizers and

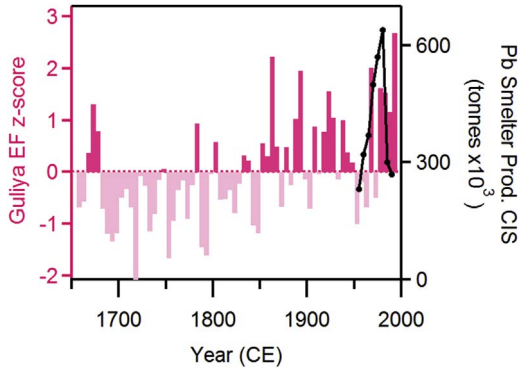


**Fig. 7.** Comparison of the Guliya Pb EF z-scores with the Pb smelter production from the CIS countries (HYDE, 2006b).

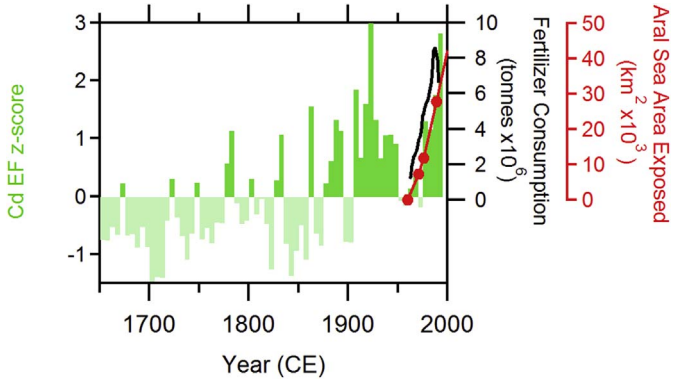


**Fig. 8.** Comparison of the Guliya Cd EF z-scores with the phosphate fertilizer consumption (FAO, 2016) (solid black curve) in the Soviet Union and with the Aral Sea area exposed (Micklin, 2007) (curve with filled circles).

pesticides that were used during this time to improve crop yields settled into the Aral Sea basin (Micklin, 1988, 2007; Issanova et al., 2015). The Cd and Pb enrichments in Guliya coincides with the onset of CIS phosphate fertilizer consumption and with the desiccation of the Aral Sea (Fig. 8). The CIS phosphate fertilizer consumption decreased in 1990, while it seems that Cd and Pb in Guliya continue to increase during 1990 and 1991, suggesting that Cd and Pb may also originate from the exposed Aral seabed and/or from other sources.

Most of China's emissions are produced in the coastal regions making it unlikely for the emissions to reach Guliya which is dominated by westerlies (Tian et al., 2015). However, Kashgar and Aksu (Xinjian province), western China, have also developed rapidly with cotton agriculture as its main economic activity (Dai and Dong, 2016). Thus, phosphate fertilizers from this region could have also contributed to the Cd and Pb enrichment observed in Guliya. South Asia (India, Nepal) just like western China (Kashgar in the Xinjian province) is in the summer high frequency back trajectories of Guliya (Fig. 2) thus their emissions (e.g., fossil fuel combustion, non-ferrous metallurgy and phosphate fertilizers) likely also contributed to the Cd and Pb enrichment observed in Guliya similar to Sn since China and India have increased their consumption of fossil fuels (Fig. 5).

The multivariate factor analysis (Table A1) and cluster analysis of TEs during the 1950–1991 sub-period (Figure A5) show possible linkages between Cd and Pb. It is then possible that they originated from common sources (fossil fuel combustion, non-ferrous metal production, phosphate fertilizers, Aral seabed) from Central Asia, western China and/or South India. On the other hand, Sn is not linked to either Cd or Pb in the 1950–1991 dendrogram (Figure A5), however we cannot rule out that these three TEs share common sources as the number of anthropogenic sources and emissions in the region have increased since the 1970s.

### 3.3. North Atlantic Oscillation (NAO) influence

Enrichments of Pb, Cd, Sb, and Zn were observed during the first half of the 20th century in the Guliya ice core but between ~1940 and ~1970 their EFs and Ex decreased to pre-industrial levels despite the fact that Europe was emitting its highest atmospheric TE concentrations at this time (Pacyna et al., 2009). As previously mentioned, due to the extremely high dust concentrations of the Guliya ice core, non-crustal contributions may be overwhelmed and may not be as easily detected as in other ice cores, however dust concentrations during this period remain at average levels. Atmospheric circulation patterns may have played an important role during this period.

Guliya receives most of the dust particles during winter, when the westerlies are dominant. The North Atlantic Oscillation (NAO) plays a significant role in the atmospheric circulation in the Northern Hemisphere (Hurrell, 1995) influencing its climate (e.g., precipitation, air temperature, wind speed and direction) (Marshall et al., 2001; Yu and Zhou, 2004). Impacts of the NAO extend well beyond the North Atlantic and Europe as NAO variability has been shown to affect Middle East precipitation (Cullen and de Menocal, 2000; Cullen et al., 2002) and East Asia temperatures (Li et al., 2008). The NAO influence on East Asia temperatures stems from a Rossby wave train in the upper atmosphere initiated over the North Atlantic and leading to stronger cyclonic flow in northern China (Li et al., 2008). The strength and position of this cyclone modulates the strength of the westerlies over the TP, such that stronger westerlies and a cooling effect in central Tibet have been associated with a positive NAO (Wang et al., 2003; Li et al., 2005; Zhang et al., 2015b). In the Eastern Tien Shan, the Cd and Ba concentration ice core records showed a negative correlation with the winter NAO index (Wang et al., 2016).

In order to determine if the TEs enrichments observed in the Guliya ice core are associated with the NAO, the winter NAO index is compared (Fig. 5) with the Pb-Cd-Sb-Zn EF composite (EF z-score). The TE enrichments observed in Guliya during the late 19th century and early 20th century coincide with a positive NAO phase whereas the TE enrichment decrease to pre-industrial levels during the ~1940 to 1970 period coincides with the negative winter NAO phase. Also, TEs (Sn, Cd, and Pb) enrichments detected after ~1965 (Sn) and 1975 (Cd, Pb), are in concert with the strong NAO positive phase after the 1970s, suggesting an increase in the transport of pollutants from western countries to Guliya from ~1965(75) to 1991.

The significant positive correlation between TEs enrichments and the winter NAO index suggests that either pollutants are transported from western countries (e.g., Europe) to Guliya by stronger westerlies via the Rossby wave train during NAO positive phases, or that the detection of TEs enrichments can be affected by changes in regional factors such as zonal wind strength/velocity, dust transport, temperature, and precipitation driven by the NAO. Further studies are needed to determine the mechanism(s) by which the TE enrichments and the NAO are correlated in the Guliya ice core.

## 4. Conclusions

This study presents the first multi-century trace element record from the northwestern Tibetan Plateau. The ice core contains an extremely high concentration of dust compared to other ice cores from the region. A thorough analysis was conducted to detect TE enrichments and two independent approaches were utilized (EF and Ex concentration). The Guliya TE records clearly show two distinct periods pre- and post-1850. The pre-1850 period shows crustal contributions primarily while enrichments of Pb, Cd, Sb, Zn, and Sn are observed after the 1850s. Enrichments of Pb, Cd, Sb, and Zn in Guliya between 1850 and 1950 can be attributed primarily to coal combustion emissions from western countries (Europe) since they were the main source during that period. Anthropogenic TE sources/regions of post-1950s Pb, Cd, and Sn enrichments are more difficult to determine since the number of anthropogenic emission sources/regions has increased worldwide. It is likely that regional emissions (fossil fuel combustion, mining/smelting, fertilizers) from Central Asia, and probably from Kashgar in western China, and South Asia (India, Nepal) could be the source of the TE enrichments (Cd, Pb, Sn) observed in Guliya after ~1970. The TEs enrichments correlate positively with the winter NAO index suggesting that non-crustal TEs mainly originated from countries west of Guliya. This could be further investigated by extending the TE records presented here from 1991 to 2015, a time period in which China's and India's emissions have increased exponentially. An ice core drilled in 2015 on the Guliya ice cap may provide this opportunity in the future.

## Acknowledgments

This work was funded by the NSF Atmospheric Chemistry Program (award 1149239) and the NSF Paleoclimate Program (award 1502919). The Guliya drilling project was funded by the NSF's Office of Climate Dynamics and the Division of Polar Programs (ATM-8519794, ATM-89116635, and DPP-9014931), the National Geographic Society (3323-86, 4309-90, and 4522-91), The Ohio State University, and the State Committee of Science and Technology and the National Natural Science Foundation of China. We thank all the participants of the Guliya 1992 field expedition. We also thank Anja Eichler, Björn Grigholm, Shugui Hou, Michael Krachler, Joseph McConnell, and Margit Schwikowski for making their TE data available. We thank Stacy Porter for valuable NAO discussions and for her help editing the manuscript and Henry Brecher and Ellen Mosley-Thompson for improving the English. This is the Byrd Polar and Climate Research Center contribution # 1574.

## Appendix A. Supplementary data

The data presented in this work are archived at the National Oceanic and Atmospheric Administration World Data Center-A for Paleoclimatology: ftp://ftp.ncdc.noaa.gov/pub/data/paleo/icecore/trop/guliya/

Supplementary data related to this article can be found at http://dx.doi.org/10.1016/j.atmosenv.2017.11.040.

## References

Bao, K., Xia, W., Lu, X., Wang, G., 2010. Recent atmospheric lead deposition recorded in an ombrotrophic peat bog of Great Hinggan Mountains, Northeast China, from $^{210}$Pb and $^{137}$Cs dating. J. Environ. Radioact. 101 (9), 773–779.

Bao, K., Shen, J., Wang, G., Roux, G., 2015. Atmospheric deposition history of trace metals and metalloids for the last 200 years recorded by three peat cores in Great hinggan Mountain, Northeast China. Atmosphere 6 (3), 380–409.

Barbante, C., Schwikowski, M., Döring, T., Gäggeler, H.W., Schotterer, U., Tobler, L., Van de Velde, K., Ferrari, C., Cozzi, G., Turetta, A., Rosman, K., Bolshov, M., Capodaglio, G., Cescon, P., Boutron, C., 2004. Historical record of European emissions of heavy metals to the atmosphere since the 1650s from alpine snow/ice cores drilled near Monte Rosa. Environ. Sci. Technol. 38, 4085–4090.

Beaudon, E., Gabrielli, P., Sierra-Hernández, M.R., Wegner, A., Thompson, L.G., 2017. Central Tibetan Plateau atmospheric trace metals contamination: a 500-year record from the Puruogangri ice core. Sci. Total Environ. 601–602, 1349–1363.

Bond, T.C., Bhardwaj, E., Dong, R., Jogani, R., Jung, S., Roden, C., Streets, D.G., Trautmann, N.M., 2007. Historical emissions of black and organic carbon aerosol from energy-related combustion, 1850–2000. Glob. Biogeochem. Cycles 21 (2).

BP, 2016. British Petroleum (BP) Statistical Review of World Energy. [9/20/2016]. .

Bradley, R.S., 2015. Paleoclimatology : Reconstructing Climates of the Quaternary.

Candelone, J.-P., Hong, S., Boutron, C.F., 1994. An improved method for decontaminating polar snow or ice cores for heavy metal analysis. Anal. Chim. Acta 299, 9–16.

Candelone, J.-P., Hong, S., Pellone, C., Boutron, C., 1995. Post-industrial revolution changes in large-scale atmospheric pollution of the Northern Hemisphere by heavy metals as documented in central Greenland snow and ice. J. Geophys. Res. 100, 16,605–616,616.

Cooke, C.A., Bindler, R., 2015. Lake sediment records of preindustrial metal pollution. In: In: Blais, J., Rosen, M., Smol, J. (Eds.), Environmental Contaminants. Developments in Paleoenvironmental Research, vol. 18. Springer, Dordrecht, pp. 101–119.

Cullen, H.M., de Menocal, P.B., 2000. North Atlantic influence on Tigris–Euphrates streamflow. Int. J. Climatol. 20 (8), 853–863.

Cullen, H.M., Kaplan, A., Arkin, P.A., de Menocal, P.B., 2002. Impact of the North Atlantic Oscillation on Middle Eastern climate and streamflow. Clim. Chang. 55 (3), 315–338.

Dai, J., Dong, H., 2016. Farming and Cultivation Technologies of Cotton in China. Cotton

Research. I. Abdurakhmonov, InTech.
Davis, M.E., 2002. Climatic Interpretations of Eolian Dust Records from Low-latitude, High-altitude Ice Cores. Ph.D. Dissertation. The Ohio State University.
Duce, R.A., Hoffman, G.L., Zoller, W.H., 1975. Atmospheric trace metals at remote Northern and Southern Hemisphere sites: pollution or natural? Science 187 (4171), 59–61.
Eichler, A., Tobler, L., Eyrikh, S., Gramlich, G., Malygina, N., Papina, T., Schwikowski, M., 2012. Three centuries of eastern European and Altai lead emissions recorded in a Belukha ice core. Environ. Sci. Technol. 46 (8), 4323–4330.
Eichler, A., Tobler, L., Eyrikh, S., Malygina, N., Papina, T., Schwikowski, M., 2014. Ice-core based assessment of historical anthropogenic heavy metal (Cd, Cu, Sb, Zn) emissions in the Soviet Union. Environ. Sci. Technol. 48, 2635–2642.
FAO, 2016. Food and agricultural organization of the United Nations. Phosphate Fertil. Consum [4/13/2016].
Ferrat, M., Weiss, D.J., Dong, S., Large, D.J., Spiro, B., Sun, Y., Gallagher, K., 2012. Lead atmospheric deposition rates and isotopic trends in asian dust during the last 9.5 Kyr recorded in an ombrotrophic peat bog on the eastern Qinghai-Tibetan plateau. Geochim. Cosmochim. Acta 82, 4–22.
Gabrielli, P., Cozzi, G., Torcini, S., Cescon, P., Barbante, C., 2008. Trace elements in winter snow of the Dolomites (Italy): a statistical study of natural and anthropogenic contributions. Chemosphere 72, 1504–1509.
Gabrielli, P., Hardy, D.R., Kehrwald, N., Davis, M., Cozzi, G., Turetta, C., Barbante, C., Thompson, L.G., 2014. Deglaciated areas of Kilimanjaro as a source of volcanic trace elements deposited on the ice cap during the late Holocene. Quat. Sci. Rev. 93, 1–10.
Gabrielli, P., Vallelonga, P., 2015. Contaminant records in ice cores. In: In: Blais, J., Rosen, M., Smol, J. (Eds.), Environmental Contaminants. Developments in Paleoenvironmental Research, vol. 18. Springer, Dordrecht, pp. 393–430.
Grigholm, B., Mayewski, P.A., Kang, S., Zhang, Y., Morgenstern, U., Schwikowski, M., Kaspari, S., Aizen, V., Aizen, E., Takeuchi, N., Maasch, K.A., Birkel, S., Handley, M., Sneed, S., 2015. Twentieth century dust lows and the weakening of the westerly winds over the Tibetan Plateau. Geophys. Res. Lett. 42, 2434–2441.
Grigholm, B., Mayewski, P.A., Aizen, V., Kreutz, K., Wake, C.P., Aizen, E., Kang, S., Maasch, K.A., Handley, M.J., Sneed, S.B., 2016. Mid-twentieth century increases in anthropogenic Pb, Cd and Cu in central Asia set in hemispheric perspective using Tien Shan ice core. Atmos. Environ. 131, 17–28.
Hansson, S., Bindler, R., De Vleeschouwer, F., 2015. Using peat records as natural archives of past atmospheric metal deposition. In: In: Blais, J., Rosen, M., Smol, J. (Eds.), Environmental Contaminants. Developments in Paleoenvironmental Research, vol. 18. Springer, Dordrecht, pp. 323–354.
Hong, S., Lee, K., Hou, S., Hur, S.D., Ren, J., Burn, L.J., Rosman, K.J.R., Barbante, C., Boutron, C.F., 2009. An 800-year record of atmospheric As, Mo, Sn, and Sb in central Asia in high-altitude ice cores from Mt. Qomolangma (Everest), Himalayas. Environ. Sci. Technol. 43, 8060–8065.
Hurrell, J.W., 1995. Decadal trends in the North Atlantic Oscillation: regional temperatures and precipitation. Science 269 (5224), 676–679.
Hurrell, J.W., 2003. NAO Index Data provided by the Climate Analysis Section. NCAR, Boulder, USA Updated Regularly. [04 July 2017].
HYDE, 2006a. History Database of the Global Environment. Hard and Brown Coal Production Estimates. [4/12/2016]. .
HYDE, 2006b. History Database of the Global Environment. Metal Production Data. [2/16/2017]. .
Indoitu, R., Orlovsky, L., Orlovsky, N., 2012. Dust storms in central Asia: spatial and temporal variations. J. Arid. Environ. 85, 62–70.
Issanova, G., Abuduwaili, J., Galayeva, O., Semenov, O., Bazarbayeva, T., 2015. Aeolian transportation of sand and dust in the Aral Sea region. Int. J. Environ. Sci. Technol. 12 (10), 3213–3224.
Jin, Z., Han, Y., Chen, L., 2010. Past atmospheric Pb deposition in lake Qinghai, northeastern Tibetan Plateau. J. Paleolimnol. 43 (3), 551–563.
Kang, S., Huang, J., Wang, F., Zhang, Q., Zhang, Y., Li, C., Wang, L., Chen, P., Sharma, C.M., Li, Q., Sillanpää, M., Hou, J., Xu, B., Guo, J., 2016. Atmospheric mercury depositional chronology reconstructed from lake sediments and ice core in the Himalayas and Tibetan Plateau. Environ. Sci. Technol. 50 (6), 2859–2869.
Kaspari, S.D., Mayewski, P.A., Handley, M., Osterberg, E., Kang, S., Sneed, S.B., Hou, S., Qin, D., 2009. Recent increases in atmospheric concentrations of Bi, U, Cs, S and Ca from a 350-year Mount Everest ice core record. J. Geophys. Res. 114, D04302.
Kokaly, R.F., King, T.V.V., Hoefen, T.M., Dudek, K.B., Livo, K.E., 2011. Surface Materials Map of Afghanistan: Carbonates, Phyllosilicates, Sulfates, Altered Minerals, and Other Materials. U.S. Geological Survey Scientific Investigations Map 3152–A. .
Krachler, M., Zheng, J., Koerner, R., Zdanowicz, C., Fisherb, D., Shotyk, W., 2005. Increasing atmospheric antimony contamination in the Northern Hemisphere: snow and ice evidence from Devon Island, Arctic Canada. J. Environ. Monit. 2005, 1169–1176.
Kuhlmann, J., Quaas, J., 2010. How can aerosols affect the Asian summer monsoon? Assessment during three consecutive pre-monsoon seasons from Calipso satellite data. Atmos. Chem. Phys. 10 4673–4668.
Kylander, M.E., Klaminder, J., Bindler, R., Weiss, D.J., 2010. Natural lead isotope variations in the atmosphere. Earth Planet. Sc. Lett. 290 (1), 44–53.
Lavanchy, V.M.H., Gäggeler, H.W., Schotterer, U., Schwikowski, M., Baltensperger, U., 1999. Historical record of carbonaceous particle concentrations from a European high-alpine glacier (Colle Gnifetti, Switzerland). J. Geophys. Res. Atmos. 104 (D17), 21227–21236.
Le Callonnec, L., Person, A., Renard, M., Létolle, R., Nebout, N., Ben Khelifa, L., Rubanov, I., 2005. Preliminary data on chemical changes in the Aral Sea during low-level periods from the last 9000 years. C. R. Geosci. 337 (12), 1035–1044.
Lee, K., Hur, S.D., Hou, S., Burn-Nunes, L.J., Hong, S., Barbante, C., Boutron, C.F., Rosman, K.J., 2011. Isotopic signatures for natural versus anthropogenic Pb in high-altitude Mt. Everest ice cores during the past 800 years. Sci. Total Environ. 412–413, 194–202.
Li, C., Kang, S., Zhang, Q., 2009. Elemental composition of Tibetan Plateau top soils and its effect on evaluating atmospheric pollution transport. Environ. Pollut. 157, 2261–2265.
Li, C., Bosch, C., Kang, S., Andersson, A., Chen, P., Zhang, Q., Cong, Z., Chen, B., Qin, D., Gustafsson, Ö., 2016. Sources of black carbon to the Himalayan–Tibetan Plateau glaciers. Nat. Commun. 7, 12574.
Li, J., Yu, R., Zhou, T., Wang, B., 2005. Why is there an early spring cooling shift downstream of the Tibetan Plateau? J. Clim. 18 (22), 4660–4668.
Li, J., Yu, R., Zhou, T., 2008. Teleconnection between NAO and climate downstream of the Tibetan Plateau. J. Clim. 21 (18), 4680–4690.
Li, Z., Yao, T., Tian, L., Xu, B., Li, Y., 2006. Atmospheric Pb variations in central Asia since 1955 from Muztagata ice core record, Eastern Pamirs. Chin. Sci. Bull. 51 (16), 1996–2000.
Liu, Y., Hou, S., Hong, S., Hur, S.D., Lee, K., Wang, Y., 2011. High-resolution trace element records of an ice core from the eastern Tien Shan, Central Asia, since 1953 AD. J. Geophys. Res. 116, D12307.
Marshall, J., Kushnir, Y., Battisti, D., Chang, P., Czaja, A., Dickson, R., Hurrell, J., McCartney, M., Saravanan, R., Visbeck, M., 2001. North Atlantic climate variability: phenomena, impacts and mechanisms. Int. J. Climatol. 21 (15), 1863–1898.
Martínez Cortizas, A., Peiteado Varela, E., Bindler, R., Biester, H., Cheburkin, A., 2012. Reconstructing historical Pb and Hg pollution in NW Spain using multiple cores from the Chao de Lamoso bog (Xistral Mountains). Geochim. Cosmochim. Acta 82 (Suppl. C), 68–78.
Martínez Cortizas, A., García-Rodeja Gayoso, E., Weiss, D., 2002. Peat bog archives of atmospheric metal deposition. Sci. Total Environ. 292 (1), 1–5.
Marx, S.K., McGowan, H.A., 2010. Long-distance transport of urban and industrial metals and their incorporation into the environment: sources, transport pathways and historical trends. In: Zereini, F., Wiseman, C.L.S. (Eds.), Urban Airborne Particulate Matter. Origin, Chemistry, Fate and Health Impacts. Springer, Berlin, pp. 103–123.
Marx, S.K., Rashid, S., Stromsoe, N., 2016. Global-scale patterns in anthropogenic Pb contamination reconstructed from natural archives. Environ. Pollut. 213 (2), 283–298.
Maussion, F., Scherer, D., Mölg, T., Collier, E., Curio, J., Finkelnburg, R., 2014. Precipitation seasonality and variability over the Tibetan Plateau as resolved by the high Asia reanalysis. J. Clim. 27 (5), 1910–1927.
McConnell, J.R., Lamorey, G.W., Hutterli, M.A., 2002. A 250-year high-resolution record of Pb flux and crustal enrichment in central Greenland. Geophys. Res. Lett. 29 (23) 45–41-45-44.
McConnell, J.R., Edwards, R., 2008. Coal burning leaves toxic heavy metal legacy in the Arctic. Proc. Natl. Acad. Sci. U. S. A. 105, 12140–12144.
Merian, E., Anke, M., Ihnat, M., Stoeppler, M. (Eds.), 2004. Elements and Their Compounds in the Environment. Occurrence, Analysis and Biological Relevance. Wiley-VCH.
Micklin, P., 2007. The Aral Sea disaster. Annu. Rev. Earth Planet. Sci. 35 (1), 47–72.
Micklin, P.P., 1988. Desiccation of the Aral Sea: a water management disaster in the Soviet Union. Science 241 (4870), 1170–1176.
Miller, J.C., Miller, J.N., 2010. Statistics and Chemometrics for Analytical Chemistry. Pearson Education Limited, New York, Ellis Horwood.
Novakov, T., Ramanathan, V., Hansen, J.E., Kirchstetter, T.W., Sato, M., Sinton, J.E., Sathaye, J.A., 2003. Large historical changes of fossil-fuel black carbon aerosols. Geophys. Res. Lett. 30 (6).
Nriagu, J.O., Pacyna, J.M., 1988. Quantitative assessment of worldwide contamination of air, water and soils by trace metals. Nature 333 (6169), 134–139.
Nriagu, J.O., 1989a. Natural versus anthropogenic emissions of trace metals to the atmosphere. In: Pacyna, J., Ottar, B. (Eds.), Control and Fate of Atmospheric Trace Metals. Kluwer Academic Publishers, pp. 3–13.
Nriagu, J.O., 1989b. A global assessment of natural sources of atmospheric trace metals. Lett. Nat. 338, 47–49.
Numaguti, A., 1999. Origin and recycling processes of precipitating water over the Eurasian continent: experiments using an atmospheric general circulation model. J. Geophys. Res. Atmos. 104 (D2), 1957–1972.
Ohmsen, G.S., 2001. Characterization of fugitive material within a primary lead smelter. J. Air Waste Manag. Assoc. 51 (10), 1443–1451.
Olendrzynski, K., Anderberg, S., Bartnicki, Jerzy, Pacyna, J., Stigliani, W., 1996. Atmospheric emissions and depositions of Cadmium, Lead, and Zinc in Europe during the period 1955-1987. Environ. Rev. 4, 300–320.
Pacyna, J.M., Pacyna, E.G., 2001. An assessment of global and regional emissions of trace metals to the atmosphere from anthropogenic sources worldwide. Environ. Rev. 9, 269–298.
Pacyna, J.M., Pacyna, E.G., Aas, W., 2009. Changes of emissions and atmospheric deposition of mercury, lead, and cadmium. Atmos. Environ. 43 (1), 117–127.
Qian, W., Quan, L., Shi, S., 2002. Variations of the dust storm in China and its climatic control. J. Clim. 15, 1216–1229.
Quinn, T.L., Ondov, J.M., 1998. Influence of temporal changes in relative humidity on dry deposition velocities and fluxes of aerosol particles bearing trace elements. Atmos. Environ. 32 (20), 3467–3479.
Reddy, M.S., Basha, S., Joshi, H.V., Jha, B., 2005. Evaluation of the emission characteristics of trace metals from coal and fuel oil fired power plants and their fate during combustion. J. Hazard. Mater 123 (1–3), 242–249.
Rolph, G., Stein, A., Stunder, B., 2017. Real-time environmental applications and display system: READY. Environ. Model. Softw. 95, 210–228.
Schettler, G., Oberhänsli, H., Stulina, G., Mavlonov, A.A., Naumann, R., 2013. Hydrochemical water evolution in the Aral Sea basin. Part I: unconfined groundwater of the Amu Darya Delta – interactions with surface water. J. Hydrol. 495, 267–284.

Schiemann, R., Lèuthi, D., Schèar, C., 2009. Seasonality and interannual variability of the westerly jet in the Tibetan Plateau region. J. Clim. 22 (11), 2940–2957.
Schwikowski, M., Barbante, C., Doering, T., Gaeggeler, H.W., Boutron, C., Schotterer, U., Tobler, L., Van de Velde, K., Ferrari, C., Cozzi, G., Rosman, K., Cescon, P., 2004. Post-17th-century changes of European lead emissions recorded in high-altitude alpine snow and ice. Environ. Sci. Technol. 38 (4), 957–964.
Shafiee, S., Topal, E., 2009. When will fossil fuel reserves be diminished? Energy Policy 37 (1), 181–189.
Shaw, D.M., Reilly, G.A., Muysson, J.R., Pattenden, G.E., Campbell, F.E., 1967. An estimate of the chemical composition of the canadian precambrian shield. Can. J. Earth Sci. 4 (5), 829–853.
Shaw, D.M., Dostal, J., Keays, R.R., 1976. Additional Estimates of continental surface precambrian shield composition in Canada. Geochim. Cosmochim. Acta 40 (1), 73–83.
Shotyk, W., 1996. Peat bog archives of atmospheric metal deposition: geochemical evaluation of peat profiles, natural variations in metal concentrations, and metal enrichment factors. Environ. Rev. Environ. Rev. 4 (2), 149–183.
Shotyk, W., Weiss, D., Appleby, P.G., Cheburkin, A.K., Frei, R., Gloor, M., Kramers, J.D., Reese, S., Van Der Knaap, W.O., 1998. History of atmospheric lead deposition since 12,370 $^{14}$C yr BP from a peat bog, Jura Mountains, Switzerland. Science 281 (5383), 1635.
Shotyk, W., Zheng, J., Krachler, M., Zdanowicz, C., Koerner, R., Fisher, D., 2005. Predominance of industrial Pb in recent snow (1994-2004) and ice (1842-1996) from Devon Island. Arct. Can. Geophys. Res. Lett. 32 (21), L21814.
Shotyk, W., Appleby, P.G., Bicalho, B., Davies, L.J., Froese, D., Grant-Weaver, I., Magnan, G., Mullan-Boudreau, G., Noernberg, T., Pelletier, R., Shannon, B., van Bellen, S., Zaccone, C., 2017. Peat bogs document decades of declining atmospheric contamination by trace metals in the Athabasca Bituminous Sands region. Environ. Sci. Technol. 51 (11), 6237–6249.
Sobanska, S., Ricq, N., Laboudigue, A., Guillermo, R., Brémard, C., Laureyns, J., Merlin, J.C., Wignacourt, J.P., 1999. Microchemical investigations of dust emitted by a lead smelter. Environ. Sci. Technol. 33 (9), 1334–1339.
Stein, A.F., Draxler, R.R., Rolph, G.D., Stunder, B.J.B., Cohen, M.D., Ngan, F., 2015. NOAA's hysplit atmospheric transport and dispersion modeling system. Bull. Am. Meteorol. Soc. 96 (12), 2059–2077.
Stone, R., 2014. Mother of all lodes. Science 345 (6198), 725–727.
Sun, J., Zhang, M., Liu, T., 2001. Spatial and temporal characteristics of dust storms in China and its surrounding regions, 1960-1999: relations to source area and climate. J. Geophys. Res. 106, 10325–10333.
Thompson, L.G., Mosley-Thompson, E., Davis, M.E., Lin, P.-N., Mikhalenko, V., Dai, J., 1995. A 1000 year ice core climate record from the Guliya ice cap, China and its relationship to global climate variability. Ann. Glaciol. 21, 175–181.
Thompson, L.G., Yao, T., Davis, M.E., Henderson, K.A., Mosley-Thompson, E., Lin, P.N., Beer, J., Synal, H.-A., Cole-Dai, J., Bolzan, J.F., 1997. Tropical climate instability: the last glacial cycle from a Qinghai-Tibetan ice core. Science 276, 1821–1825.
Thompson, L.G., Mosley-Thompson, E., Brecher, H., Davis, M., León, B., Les, D., Lin, P.N., Mashiotta, T., Mountain, K., 2006a. Abrupt tropical climate change: past and present. Proc. Natl. Acad. Sci. U. S. A. 103 (28), 10536–10543.
Thompson, L.G., Yao, T., Davis, M.E., Mosley-Thompson, E., Mashiotta, T.A., Lin, P.-N., Mikhalenko, V.N., Zagorodnov, V.S., 2006b. Holocene climate variability archived in the Puruogangri ice cap on the central Tibetan Plateau. Ann. Glaciol. 43 (1), 61–69.
Tian, H.Z., Zhu, C.Y., Gao, J.J., Cheng, K., Hao, J.M., Wang, K., Hua, S.B., Wang, Y., Zhou, J.R., 2015. Quantitative assessment of atmospheric emissions of toxic heavy metals from anthropogenic sources in China: historical trend, spatial distribution, uncertainties, and control policies. Atmos. Chem. Phys. 15, 10127–10147.
Tian, L., Masson-Delmotte, V., Stievenard, M., Yao, T., Jouzel, J., 2001. Tibetan Plateau summer monsoon northward extent revealed by measurements of water stable isotopes. J. Geophys. Res. Atmos. 106 (D22), 28081–28088.
Tian, L., Yao, T., MacClune, K., White, J.W.C., Schilla, A., Vaughn, B., Vachon, R., Ichiyanagi, K., 2007. Stable isotopic variations in west China: a consideration of moisture sources. J. Geophys. Res. 112 (D10), D10112.
Uglietti, C., Gabrielli, P., Olesik, J.W., Lutton, A., Thompson, L.G., 2014. Large variability of trace element mass fractions determined by ICP-SFMS in ice core samples from worldwide high altitude glaciers. Appl. Geochem 47, 109–121.
Uglietti, C., Gabrielli, P., Cooke, C.A., Vallelonga, P., Thompson, L.G., 2015. Widespread pollution of the south american atmosphere predates the industrial revolution by 240 Y. Proc. Natl. Acad. Sci. U. S. A. 112 (8), 2349–2354.
Wang, C., Liu, Y., Zhang, W., Hong, S., Hur, S.D., Lee, K., Pang, H., Hou, S., 2016. High-resolution atmospheric cadmium record for AD 1776–2004 in a high-altitude ice core from the eastern Tien Shan. Cent. Asia. Ann. Glaciol. 57, 265–272.
Wang, N., Thompson, L.G., Davis, M.E., Mosley-Thompson, E., Yao, T., Jianchen, P., 2003. Influence of variations in NAO and SO on air temperature over the northern Tibetan Plateau as recorded by $\delta^{18}$0 in the Malan ice core. Geophys. Res. Lett. 30 (22) 5–1-5-4.
Wang, X., Yang, H., Gong, P., Zhao, X., Wu, G., Turner, S., Yao, T., 2010. One century sedimentary records of polycyclic aromatic hydrocarbons, mercury and trace elements in the Qinghai Lake. Environ. Pollut. 158 (10), 3065–3070.
Wedepohl, K.H., 1995. The composition of the continental crust. Geochim. Cosmochim. Acta 59, 1217–1232.
Weiss, D., Shotyk, W., Appleby, P.G., Kramers, J.D., Cheburkin, A.K., 1999. Atmospheric Pb deposition since the industrial revolution recorded by five Swiss peat profiles: enrichment factors, fluxes, isotopic composition, and sources. Environ. Sci. Technol. 33 (9), 1340.
Wu, G., Xu, B., Zhang, C., Gao, S., Yao, T., 2009a. Geochemistry of dust aerosol over the eastern Pamirs. Geochim. Cosmochim. Acta 73 (4), 977–989.
Wu, G., Zhang, C., Gao, S., Yao, T., Tian, L., Xia, D., 2009b. Element composition of dust from a shallow Dunde ice core, Northern China. Glob. Planet. Change 67 (3–4), 186–192.
Xu, M., Yan, R., Zheng, C., Qiao, Y., Han, J., Sheng, C., 2004. Status of trace element emission in a coal combustion process: a review. Fuel Process. Technol. 85 (2–3), 215–237.
Yang, H., Battarbee, R.W., Turner, S.D., Rose, N.L., Derwent, R.G., Wu, G., Yang, R., 2010. Historical reconstruction of mercury pollution across the Tibetan Plateau using lake sediments. Environ. Sci. Technol. 44 (8), 2918–2924.
Yao, T., Thompson, L.G., Yang, W., Yu, W., Gao, Y., Guo, X., Yang, X., Duan, K., Zhao, H., Xu, B., Pu, J., Lu, A., Xiang, Y., Kattel, D.B., Joswiak, D., 2012. Different glacier status with atmospheric circulations in Tibetan Plateau and surroundings. Nat. Clim. Chang. 2, 663–667.
Yao, T.D., Masson-Delmotte, V., Gao, J., Yu, W.S., Yang, X.X., Risi, C., Sturm, C., Werner, M., Zhao, H.B., He, Y., Ren, W., Tian, L.D., Shi, C.M., Hou, S.G., 2013. A review of climatic controls on $\delta^{18}$O in precipitation over the Tibetan Plateau: observations and simulations. Rev. Geophys. 51 (4), 525–547.
Yu, R., Zhou, T., 2004. Impacts of winter-NAO on March cooling trends over subtropical Eurasia continent in the recent half century. Geophys. Res. Lett. 31 (12), L12204.
Zhang, Q., Kang, S., Gabrielli, P., Loewen, M., Schwikowski, M., 2015a. Vanishing high mountain glacial archives: challenges and perspectives. Environ. Sci. Technol. 49, 9499–9500.
Zhang, X.Y., Arimoto, R., Cao, J.J., An, Z.S., Wang, D., 2001. Atmospheric dust aerosol over the Tibetan Plateau. J. Geophys. Res. 106, 18471–18476.
Zhang, X., Zhibao, S., Guangyu, Z., Tuo, C., Haiyan, L., 1996. Remote mineral aerosols in Westerlies and their contributions to the Chinese loess. Sci. China 39, 134–143.
Zhang, Y., Kang, S., Zhang, Q., Grigholm, B., Kaspari, S., You, Q., Qin, D., Mayewski, P.A., Cong, Z., Huang, J., Sillanpää, M., Chen, F., 2015b. A 500 Year atmospheric dust deposition retrieved from a Mt. Geladaindong ice core in the central Tibetan Plateau. Atmos. Res. 166, 1–9.
Zhao, Y., Huang, A., Zhu, X., Zhou, Y., Huang, Y., 2013. The impact of the winter North Atlantic Oscillation on the frequency of spring dust storms over Tarim basin in northwest China in the past half-century. Environ. Res. Lett. 8, 024026.
Zheng, M., Liu, X., 2009. Hydrochemistry of salt lakes of the Qinghai-Tibet Plateau, China. Aquat. Geochem 15, 293–320.
Zoller, W.H., Gladney, E.S., Duce, R.A., 1974. Atmospheric concentrations and sources of trace metals at the South Pole. Science 183 (4121), 198–200.